

# PARSEC'S HIGH PRECISION ASTROMETRY - THE MAKING OF

B. BUCCIARELLI<sup>1</sup>, A.H. ANDREI<sup>1,2,4,5</sup>, R.L. SMART<sup>1</sup>, U. SCHIROSI<sup>1</sup>,  
M. DAPRA<sup>1</sup>, M.G. LATTANZI<sup>1</sup>, J.L. PENNA<sup>2</sup>, D.N. DA SILVA NETO<sup>3</sup>

<sup>1</sup> INAF-OATo Osservatorio Astronomico di Torino  
Strada Osservatorio 20, 10025 Pino Torinese, TO, Italy  
e-mail: bucciarelli@oato.inaf.it

<sup>2</sup> ON/MCT Observatorio Nacional, Brazil

<sup>3</sup> UEZO Universidade Estadual da Zona Oeste, Brazil

<sup>4</sup> SYRTE/OP Observatoire de Paris, France

<sup>5</sup> Observatorio do Valongo/UFRJ, Brazil

**ABSTRACT.** The core of the PARSEC (Parallaxes of Southern Extremely Cool Objects) program aims at delivering trigonometric parallaxes for over 100 brown dwarfs with an average magnitude of  $\sim 17.3$  in the  $z$  band. Stringent observing criteria and careful data treatment, endowed with the current best reference catalogues as calibrators, allow to achieve 5-mas accuracy on position, proper motion and parallactic shift. Astrometric parameters are derived by means of three different approaches, testing in such a way the robustness of the solution. The issues of CCD fringing removal, object matching and choice of the reference observation are addressed. Further observational campaigns recently undertaken to increase the size of the sample and push its average magnitude towards fainter regimes will allow to determine absolute distances of brown dwarfs down to the later T spectral sub-classes, where independent data are mostly needed for understanding their evolution.

## 1. SCIENCE DRIVERS AND PROGRAM OUTLINE

Understanding extremely low-mass stellar astrophysics is a major goal of current studies of brown dwarfs. Absolute distances are fundamental to determining model-independent temperatures for these sub-stellar objects, hence properly placing them on the color-magnitude diagram. The interpretation of the cooling sequences defined by brown dwarfs in the HR diagram is complicated by an intrinsic mass/age/luminosity degeneracy: older, more massive objects cannot be distinguished from younger, less massive ones. As a consequence, their Luminosity Function is a result of a combination of their Initial Mass Function and their Star Formation History. It appears evident that, while independent methods must be devised in order to constrain the mass/age parameters, trigonometric parallaxes are key quantities to help disentangling such a degeneracy. Ultimately, because of their large number, ubiquity and long-lasting evolution, brown dwarfs represent an especially interesting class of objects for a variety of Galactic studies. More specifically, cold brown dwarf astrophysics is particularly relevant to “hot” science topics such as

- Tests of current atmospheric and evolutionary models of extremely low-mass objects
- Changes of atmospheric processes according to temperature, chemistry, mass and age variations, and their affinity to gas giant planets atmospheres
- Contribution to the Galaxy thin disk, thick disk and halo populations and impact on the history of Galaxy formation

With these objectives in mind, the PARSEC program and its successors, NPARSEC, an ESO Large Program proposal, and IPERCOOL, a Marie Curie FP7 European Community Grant gathering the expertise in the field from Italy, England, China and Brazil, are realizing the largest homogeneous dataset comprising astrometric and astrophysical parameters of L and T dwarfs, which shall be exploited to address some of the above issues.

Until the early 2000's, parallax programs of T dwarfs were operating in a “discovery” mode, by responding to new detections of cooler and cooler temperatures, with the result of becoming biased

toward low luminosity objects (Smart 2009). More recently, new available infrared surveys, such as UKIDSS, CFBDS and WISE, have significantly increased the number of known T dwarfs, furthermore extending the spectral range to T9 and beyond. Building on these surveys' assets, our target list has been culled with the goal of providing statistically significant samples in all sub-classes, while still having the potential to rapidly follow up on newly discovered interesting objects. The PARSEC program (Andrei et al. 2011) was executed using the WFI imager (30-arcmin FOV) +  $z$  filter ( $0.964 \mu\text{m}$ ) of the ESO 2.2-m, and was concluded at the beginning of 2011 just when the NPARSEC program, concerning fainter objects, took start at the ESO NTT with the SOFI imager (5-arcmin FOV) +  $J$  filter ( $1.247 \mu\text{m}$ ). In Figures 1 and 2 the distribution of our targets as function of spectral class and magnitude is displayed.

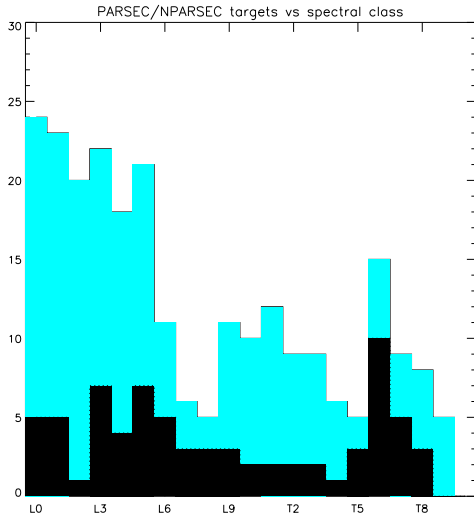


Figure 1: Distribution of PARSEC/NPARSEC targets as function of spectral class (light shadow) and, for comparison, brown dwarf parallaxes from literature data (in black)

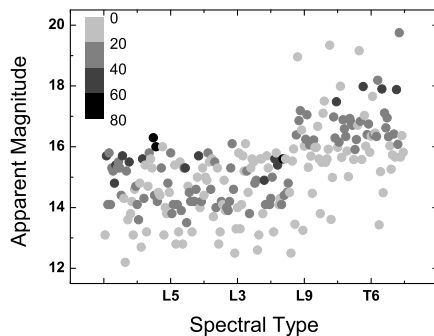


Figure 2: Targets'  $J$  magnitude vs spectral type; the gray scale indicates the object's distance in parsecs

## 2. DATA REDUCTION

We will focus here on the calibration procedures adopted for the WFI camera, since the reduction of SOFI data is still in a preliminary stage. The initial image treatment uses standard IRAF routines for bias and flat subtraction. However, fringing removal required a tailored approach. The interference fringes in the infrared images of the WFI camera are severe: an examination of the counts shows they can vary by up to 10% over the distance of a few pixels. The ideal case would be to make a fringe map for each image: since this was not feasible, our compromise was to make a nightly fringe map whenever possible. The details of our technique are given in Andrei et al. (2011). We emphasize here that a suitable subset of images scaled by their exposure time is selected to make an initial fringe map, removing in such a way most of the fringe patterns; thereafter, the same subset of pre-cleaned images is combined into a final fringe map by adopting the image mean counts as scale factor in order to take into account the sky-dependent intensity of the fringe pattern as well. Figure 3 illustrates a comparison between object centroiding errors using a standard fringe map (as provided by ESO) and ours showing a sensible improvement. All the objects identified on each CCD frame are measured using Robin, a CCD software package developed at OATo (Lanteri 1990), which estimates their centroiding  $x, y$ ; then, positions from different frames/epochs are cross-matched by means of a low-order polynomial fit, before feeding them to the astrometric model. There are presently several sky surveys that could be combined to our data to provide longer time coverage, when desirable; moreover, multi-band photometry is extremely useful to calibrate our observations, which are limited to one filter only. For this, we intend to exploit catalogs like 2MASS, SDSS, GSC-2, and possibly WISE to extend the astrometric and photometric calibrations to the full field of view, where other objects of interest also appear, with particular attention to the wide WFI CCD field. In order to match observations spanning a long time interval, where usual cone search

strategies might fail, we adopt a more sophisticated procedure which assigns higher priority to objects with low proper motion and better positional accuracy, removes matched stars and re-starts the process, also allowing for periodical signatures.

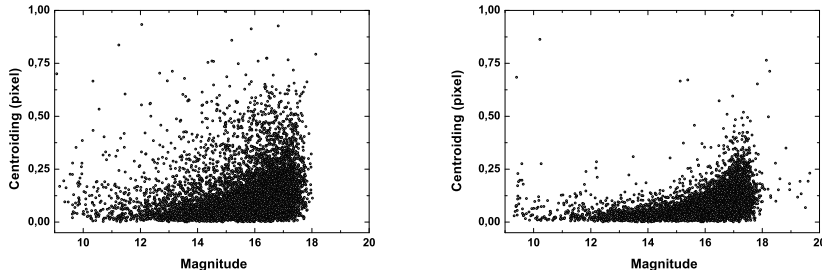


Figure 3: Image centroiding errors (in pixels) vs object magnitude with a standard fringe removal (left) and with our tailored procedure (right)

### 3. ASTROMETRIC SOLUTION

We have developed three methods for the derivation of the target’s parallax, checking in this way the robustness of the solution. The canonical approach is to express the stellar motions in equatorial standard coordinates and to build a system of equations which includes the astrometric parameters of all stars and the instrumental parameters of all frames, the latter suitably modelled by a first order polynomial. In this case, the observation equation for the longitudinal standard coordinate of a generic star on a frame  $i$  reads:

$$-x_i = a_i x_i + b_i y_i + c_i - \xi_0 - \mu_\xi(t_i - t_0) - P_{\xi_i} \pi_\xi$$

where  $(x_i, y_i)$  are the object’s image centroid,  $t_0$  a chosen reference epoch and  $P_{\xi_i}$  the parallax factor (Bucciarelli et al. 2010). The parameters to be estimated are  $\xi_0$ ,  $\mu_\xi$ ,  $\pi_\xi$ , i.e., the star position at  $t_0$ , its longitudinal proper motion and its parallax, and the instrumental coefficients  $a, b, c$  mapping each frame onto the tangential plane. We have tackled the intrinsic rank deficiency of this problem using two solution techniques: a block iterative one, which is naturally convergent without the need of constraint equations, and a direct one requiring nine additional constraints to fix the solution (Bucciarelli et al. 2010). A different approach consists in using field stars to tie all frames together and then solving for the astrometric parameters of the target star, as detailed in the following. If all frames were equivalent, an equivalent result would be obtained adopting any frame as the reference one, but despite our emphasis on image quality, adequacy and repeatability, the choice is not immaterial; therefore, we have investigated this issue using simulated data. We generated the observations of a typical PARSEC set of a patch of sky imaged twice nightly for 26 nights, with up to 800 stars per image. As we wanted to establish a guideline for the definition of the reference frame in the presence of observational errors, we disregarded systematic effects, so the fake stars have no proper motion, parallax, or movements due to the reference system. Also, the size or time interval of the frames is unimportant. On the other hand, using the outcomes of a Gaussian noise generator, stars could appear and disappear from one frame to another, centroiding errors were assigned, plus terms accounting for tilt and telescope pointing. The fake stars were placed over a regular grid so that their matching in different frames only depended on the repeatability of their position (and not on the performance of a recognition algorithm). The average value resulting from a Monte Carlo simulation of 1,000 runs are shown in Table 1. Results are given for a basis frame corresponding to the first one observed, or the densest one, or yet a fictitious *mean* frame. The poorest choice is to adopt the first frame observed. The densest and the mean frame lead to small differences, although the latter is about 10% better. Additionally, the operation of building a mean frame, though asking for additional computational effort, corresponds to an object matching task, which saves time in the following steps of data reduction.

Solution	Stars Matched	Mean Precision (")
1 <sup>st</sup> frame	257 ± 76	0.0028 ± 0.0001
Densest frame	493 ± 128	0.0026 ± 0.0001
Mean frame	527 ± 134	0.0023 ± 0.0001

Table 1: For each choice of the basis frame, the number of stars found in every frame is given, and the standard deviation of the positional adjustment for those stars.

Once the ensemble of standard coordinates  $(\xi_{t_i}, \eta_{t_i})$ ,  $t_i =$  epoch of observation, of the target star is on the same reference frame, it can be fitted with an elliptic motion modelling the parallactic effect superimposed to a linear term which accounts for the star’s transversal motion. By adopting ecliptic coordinates, and neglecting the eccentricity of the Earth’s orbit, the observation equation in  $\xi$  takes the simple form (and analogously for the  $\eta$  component)

$$\xi_{t_i}(x, y) = \pi_\xi \sin(t_i + \phi_\xi) + \mu_\xi(t_i - t_0)$$

where  $\pi_\xi$  is the object’s parallax,  $\phi_\xi$  is a phase term, and  $t_0$  the epoch of the reference frame. We note that, even if the effect of Earth eccentricity can be disregarded given the typical distances of our targets, it can be in principle computed and corrected for being a purely geometrical effect. As an example, we report the reduction of 6 years of observations (93 frames, 54 reference stars) of the high proper motion star LHS3482 (2MASS J19462386+3201021) with the three techniques giving very consistent results, as shown in Table 2. It can be noted that the quoted errors are sensibly smaller in the case of the direct method. An explanation could lie in the fact the standard deviations coming from the covariance matrix are slightly underestimated, while in the other two cases, the errors are estimated from the residuals of the fit to the target’s trajectory and could be more realistic indicators of the true errors.

Method	$\pi$ (mas)	$\mu_\alpha \cos\delta$ (mas/y)	$\mu_\delta$ (mas/y)
Block iterative	68.7 ± 4.0	458.8 ± 1.2	−391.2 ± 2.0
Direct LS	68.9 ± 0.8	457.5 ± 0.2	−390.4 ± 0.3
Ellipse fit	70.0 ± 3.2	467.7 ± 0.7	−392.0 ± 1.7

Table 2: The first two methods are variant of the canonical approach: in the first line the one used by the OATo parallax programs, in the second line a solution with all parameters derived at once using a robust least squares (LS) algorithm. The third line shows the results of a direct fit of the target star’s trajectory on the ecliptic tangential plane.

*Acknowledgements.* A.H.A. thanks CNPq grant PQ-307126/2006-0, and the PARSEC International Incoming Fellowship within the Marie Curie FP7 Programme.

#### 4. REFERENCES

- Andrei, A.H., Smart, R.L., et al. 2011, “Parallaxes of Southern Extremely Cool Objects. I. Targets, Proper Motions, and First Results”, AJ 141 p54.
- Bucciarelli, B., Andrei, A.H., Smart, R.L. et al. 2010 “Absolute Parallaxes and Proper Motions from the PARSEC Program”, in Journées 2010, Systèmes de Référence Spatio-Temporels, Paris, 22-23 September, pp. 105-108.
- Lanteri, L. 1990, Robin Software, Tech. Rep. 16, Osservatorio Astronomico di Torino.
- Smart, R.L. 2009, “Bron Dwarf Parallax Programs”, in Mem. S.A.It. Vol. 80, pp. 674-677.